J. Shanghai Jiao Tong Univ. (Sci.), 2024, 29(4): 656-666
https://doi.org/10.1007/s12204-023-2673-0

Distributed Cooperative Anti-Disturbance Control for High-Order MIMO Nonlinear Multi-Agent Systems

JIN Feiyu (金飞宇), *CHEN Longsheng** (陈龙胜), *LI Tongshuai* (李统帅), *SHI Tongxin* (石童昕)
(School of Aircraft Engineering, Nanchang Hangkong University, Nanchang 330063, China)

Abstract: To solve the synchronization and tracking problems, a cooperative control scheme is proposed for a class of higher-order multi-input and multi-output (MIMO) nonlinear multi-agent systems (MASs) subjected to uncertainties and external disturbances. First, coupled relationships among Laplace matrix, leader-following adjacency matrix and consensus error are analyzed based on undirected graph. Furthermore, nonlinear disturbance observers (NDOs) are designed to estimate compounded disturbances in MASs, and a distributed cooperative anti-disturbance control protocol is proposed for high-order MIMO nonlinear MASs based on the outputs of NDOs and dynamic surface control approach. Finally, the feasibility and effectiveness of the proposed scheme are proven based on Lyapunov stability theory and simulation experiments.
Keywords: nonlinear disturbance observer (NDO), higher-order multi-input and multi-output (MIMO) system, multi-agent system, cooperative control, disturbance suppression
CLC number: TM712, TP273 **Document code:** A

0 Introduction

Control systems have developed from centralization, decentralization, fieldbus to intelligent control. In addition, the control unit has become increasingly intelligent. Modern control systems have taken on the shape of multi-agent systems (MASs), and the control method of the systems is increasingly trending toward multi-agent cooperative control mode. Compared with individual intelligent system, MASs have the advantages of high efficiency, high reliability, flexibility, robustness and fault tolerance, as well as the ability to perform certain tasks that would be difficult for a single agent to do[1]. Nowadays, MASs are widely used in formation control[2-3], cluster control[4-5], electric networks, and sensor networks[6-8].

The main researches in the field of MASs control include formation problems[9-10], cluster problems[11], consensus problems[12-15], etc. Considering that the computation capacity and communication bandwidth of individual agent are usually limited in engineering practice, the problem of consensus control, which only requires local agents in a system by communicating with each other to achieve an overall cooperation, has received an extensive attention from researchers[16-17]. In order to further reduce the computation burden of individual agent, a problem of event-triggered consensus control about MASs was studied in Refs. [18-20], which effectively reduced the communication cost and computation burden caused by repeated communication among agents with the event-trigger scheme that was introduced in the controller. However, event-trigger scheme will cause the Zeno phenomenon sometimes, which is a situation that certain events are triggered repeatedly over a period of time, making the introduction of this scheme undesirable. To analyze the reason of Zeno phenomenon, the basic properties of the minimum event trigger interval in several event-trigger control structures were studied in Ref. [21], including the influence of external disturbances and measuring noise. In addition, the finite-time consensus problem has been widely studied in order to keep the system with a high tracking accuracy and convergence speed[22-24]. The finite-time consensus problem under switching topology condition was investigated in Refs. [25-27], and then a distributed switching cooperative control protocol was constructed that can make the system achieve finite-time consensus. However, when the initial state of the system is unknown, the upper bound of the convergence time cannot be calculated. In order to overcome the aforementioned limitation, the fixed time consensus problem based on MASs with non-linear dynamics

Received: 2023-07-21 **Accepted:** 2023-08-05
Foundation item: the National Natural Science Foundation of China (No. 61963029), and the Jiangxi Provincial Natural Science Foundation (Nos. 20224BAB202027 and 20232ACB202007)
***E-mail:** lschen2008@163.com

was studied in Refs. [28-29], which excluded the influence of the initial state of the system for the global stable convergence time. It is worth mentioning that the above studies are based on single-input and single-output (SISO) system models, while multi-input and multi-output (MIMO) characteristic is widely present in agent models of engineering practice, such as unmanned aircraft (UAV)[30], and unmanned vessel[31]. Therefore, the consensus problem for a class of MIMO multi-agent systems in the presence of input saturation, specified time and unknown dead zone was investigated in Refs. [32-34], respectively. Although positive results have been obtained in above studies, the design process, structure and stability proof of the controller became complicated while satisfying various performances of the system.

The application scenario of MASs always surrounded by various unknown disturbances is extensive and complex, while the tracking accuracy of the system is important in engineering practice. Fortunately, disturbance observer, which is physically significant and simple in structure, has been proven to be an effective method to deal with system uncertainties and unknown external disturbances[35]. In Ref. [35], a distributed disturbance observer was constructed for a class of nonlinear MASs with external disturbances and switching topology to estimate the disturbances suffered by followers, then a distributed consensus control protocol based on the observer was proposed. To address a class of nonlinear systems with parameter uncertainties, and matched and mismatched disturbances, a disturbance observer with only one tuning parameter was designed in Ref. [36] to attain the disturbance compensation, and then by combining it with command filter technique and adaptive control, a command filtering controller with adaptive-gain auxiliary systems was developed, achieving an asymptotic tracking. However, it is worth noting that the above studies of MASs have been limited to first- or second-order system models. In fact, many systems of objects are modeled with higher order dynamics in nature and engineering; for example, single linkage flexible joint robotic arm systems and pendulum arm systems are modeled with fourth and third order dynamics respectively[37]. For higher-order systems, backstepping method makes the design of the controller very standard, and its advantages in improving the quality of system transition process maintain the stability and error convergence, making it one of the most effective methods for dealing with complex nonlinear system control problems[38]. For a class of high-order MIMO nonlinear systems with unmeasurable states, an adaptive fuzzy output feedback control protocol has been constructed in Ref. [39] using the backstepping method. However, traditional backstepping method produces a "computational explosion" problem when resolving the higher order derivatives of the virtual control law[40]. Dynamic surface control (DSC) effectively solves this problem by estimating the virtual control law and derivative at each step through the use of first-order filter[41-44]. In Ref. [41], the principle and technical details of DSC were described, furthermore, nonlinear filter was introduced in the controller design[42], and then the proposed adaptive dynamic surface control scheme solved the "computational explosion" problem in the control of n-degrees of freedom hydraulic manipulators. Nevertheless, it is not easy to apply existing research results based on first- or second-order system models to higher-order MASs. The challenge lies in the stability of the Lyapunov function solution and the control singularity problem in the direct extension of existing methods[45].

Considering the above discussion and analysis, the research model in this paper is extended to a class of uncertain high-order MIMO nonlinear MASs with uncertainty and unknown external disturbances combining with engineering practice, and then a distributed cooperative anti-disturbance scheme is proposed. The main contribution and work of this paper are as follows: ① Coupled relationships among Laplace matrix, leader-following adjacency matrix and consensus error are analyzed based on undirected graphs, which make the structure of the designed control protocol comparatively simple; ② Nonlinear disturbance observer (NDO) is designed to suppress the effects of uncertainties and external dynamic disturbances on the performance of closed-loop systems, and a distributed cooperative anti-disturbance control protocol is developed based on DSC for high-order MIMO nonlinear MASs to achieve a real-time tracking of leader output signals; ③ An appropriate Lyapunov function is designed to demonstrate the stability of the closed-loop system, and the effectiveness of the designed control protocol is verified by numerical simulation.

1 Preliminaries and Problem Formulation

1.1 Algebraic Graph Theory

The communication topology among N ($N \geqslant 2$) agents can be described by undirected graphs and directed graphs. Assuming that each node corresponds to an agent, the topology of N nodes is represented by an undirected graph $\mathcal{G} = (\mathcal{V}, \mathcal{E}, \boldsymbol{A})$, where $\mathcal{V} = (1, 2, \cdots, N)$ is a nonempty set of nodes, $\mathcal{E} = \{(i, j), i, j \in \mathcal{V}\}$ is the set of edges formed by ordered edges of all nodes, and $\boldsymbol{A} = [a_{ij}] \in \mathbf{R}^{N\times N}$ is the weighted adjacency matrix. If $(i, j) \in \mathcal{E}$, then node i and node j can communicate with each other and $a_{ij} > 0$; otherwise, $a_{ij} = 0$. If $\mathcal{G}$ has no loops, then $a_{ii} = 0$. Define $b_i = \sum_{j}^{N} a_{ij}$, $j \neq i$ to be the weighted

in-degree of node i and $\boldsymbol{B}=\mathrm{diag}(b_1,b_2,\cdots,b_N)$ as the in-degree matrix. Then, the Laplacian matrix is defined by $\boldsymbol{L}=\boldsymbol{B}-\boldsymbol{A}$. Assuming that there is a virtual leader 0 among the MASs, $\boldsymbol{H}=\mathrm{diag}(h_1,h_2,\cdots,h_N)$ is defined as the leader-follower adjacency matrix, and h_i is the contact weight between agent i and the virtual leader. When agent i and the virtual leader can communicate, $h_i>0$; otherwise, $h_i=0$. For the communication topology graph shown in Fig. 1, assuming that the weights of all edges are 1, the in-degree matrix $\boldsymbol{B}=\mathrm{diag}(1,2,2,1)$ is obtained, and the adjacency weight matrix $\boldsymbol{A}$ and Laplace matrix $\boldsymbol{L}$ are as follows:

$$\boldsymbol{A}=\begin{bmatrix}0&1&0&0\\1&0&1&0\\0&1&0&1\\0&0&1&0\end{bmatrix},\quad \boldsymbol{L}=\begin{bmatrix}1&-1&0&0\\-1&2&-1&0\\0&-1&2&-1\\0&0&-1&1\end{bmatrix}.$$

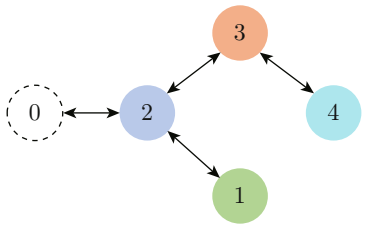

Fig. 1 Communication topology diagram

1.2 Problem Statement

Considering a class of high-order MIMO nonlinear MASs with N nodes, the dynamic equation of agent i is given as follows:

$$\left.\begin{aligned}&\dot{\boldsymbol{x}}_i^q=\boldsymbol{F}_i^q(\bar{\boldsymbol{x}}_i^q)+\boldsymbol{G}_i^q(\bar{\boldsymbol{x}}_i^q)\boldsymbol{x}_i^{q+1}+\boldsymbol{D}_i^q(\bar{\boldsymbol{x}}_i^q,t)\\&q=1,2,\cdots,n-1\\&\dot{\boldsymbol{x}}_i^n=\boldsymbol{F}_i^n(\bar{\boldsymbol{x}}_i^n)+\boldsymbol{G}_i^n(\bar{\boldsymbol{x}}_i^n)\boldsymbol{u}_i+\boldsymbol{D}_i^n(\bar{\boldsymbol{x}}_i^n,t)\\&\boldsymbol{y}_i=\boldsymbol{x}_i^1\end{aligned}\right\},\tag{1}$$

where, $i=1,2,\cdots,N$, $\bar{\boldsymbol{x}}_i^q=[\boldsymbol{x}_i^1\ \ \boldsymbol{x}_i^2\ \ \cdots\ \ \boldsymbol{x}_i^q]^{\mathrm{T}}$, $\boldsymbol{x}_i^q=[x_{i1}^q\ \ x_{i2}^q\ \ \cdots\ \ x_{im}^q]^{\mathrm{T}}$ is the state vector of agent i; $\boldsymbol{u}_i\in\mathbf{R}^s$, and $\boldsymbol{y}_i=\boldsymbol{x}_i^1\in\mathbf{R}^m$ denote the control input and output of system (1), respectively; $\boldsymbol{F}_i^q(\bar{\boldsymbol{x}}_i^q)\in\mathbf{R}^m$, $\boldsymbol{G}_i^q(\bar{\boldsymbol{x}}_i^q)\in\mathbf{R}^{m\times m}$ and $\boldsymbol{G}_i^n(\bar{\boldsymbol{x}}_i^n)\in\mathbf{R}^{m\times s}$ are known smooth nonlinear functions; $\boldsymbol{D}_i^q(\bar{\boldsymbol{x}}_i^q,t)=\Delta\boldsymbol{F}_i^q(\bar{\boldsymbol{x}}_i^q)+\boldsymbol{d}_i^q(t)$ is the unknown compound disturbance. Additionally, $\Delta\boldsymbol{f}_i^q(\bar{\boldsymbol{x}}_i^q)$ and $\boldsymbol{d}_i^q(\bar{\boldsymbol{x}}_i^q,t)$, $q=1,2,\cdots,n$ denote the uncertainties and external time-varying disturbances of system (1), respectively.

The objective is to develop a distributed cooperative control protocol for the high-order MIMO nonlinear MAS (1), which can guarantee that each agent's output signal $\boldsymbol{y}_i$ in the MASs can track the virtual leader output signal $\boldsymbol{y}^{\mathrm{r}}$ with consensus errors converging to the neighborhood of zero, and all signals in closed-loop system are eventually consistently bounded.

To facilitate achieving above objectives, the following assumptions and lemmas are given.

Assumption 1[38] There is a virtual leader 0 with output $\boldsymbol{y}^{\mathrm{r}}$ in high-order MIMO nonlinear MASs, whose state is measurable and sensible for some followers, and the output signal of the virtual leader satisfies: $\boldsymbol{y}^{\mathrm{r}}$, $\dot{\boldsymbol{y}}^{\mathrm{r}}$ and $\ddot{\boldsymbol{y}}^{\mathrm{r}}$ are bounded; that is, there exists an unknown constant $B_0>0$ such that $\Pi_0=\{(\boldsymbol{y}^{\mathrm{r}},\dot{\boldsymbol{y}}^{\mathrm{r}},\ddot{\boldsymbol{y}}^{\mathrm{r}}):\ \|\boldsymbol{y}^{\mathrm{r}}\|^2+\|\dot{\boldsymbol{y}}^{\mathrm{r}}\|^2+\|\ddot{\boldsymbol{y}}^{\mathrm{r}}\|^2\leqslant B_0\}$, where $\|\cdot\|$ denotes the Frobenius norm of a matrix or the Euclidean norm of a vector.

Assumption 2[46] For the high-order MIMO nonlinear MAS (1), the derivative of compound disturbance $\boldsymbol{D}_i^q$ is bounded, that is, there exists unknown constant $\beta_i^q>0$ such that $\left\|\dot{\boldsymbol{D}}_i^q\right\|\leqslant\beta_i^q$, $q=1,2,\cdots,n$.

Assumption 3[47] For the high-order MIMO nonlinear MAS (1), the inverse matrix of $\boldsymbol{G}_i^q\in\mathbf{R}^{m\times m}$ exists, $q=1,2,\cdots,n-1$, and the generalized inverse matrix of $\boldsymbol{G}_i^n\in\mathbf{R}^{m\times s}$ exists. In addition, there exists a positive constant $\bar{\lambda}_i^q$ such that $\lambda_{\max}(\boldsymbol{G}_i^q(\boldsymbol{G}_i^q)^{\mathrm{T}})\leqslant\bar{\lambda}_i^q$, $q=1,2,\cdots,n$.

Lemma 1[48] Considering bounded initial conditions, if there exists a C^q continuous and positive definite Lyapunov function $V(\boldsymbol{x})$ satisfying $\pi_1(\|\boldsymbol{x}\|)\leqslant V(\boldsymbol{x})\leqslant\pi_2(\|\boldsymbol{x}\|)$ such that $\dot{V}(\boldsymbol{x})\leqslant-\kappa V(\boldsymbol{x})+c$, where $\pi_1,\pi_2:\mathbf{R}^m\to\mathbf{R}$ are class K functions, and κ and c are positive constants, then the system state $\boldsymbol{x}(t)$ is eventually consistently bounded.

2 Distributed Cooperative Anti-Disturbance Control Design

From the coordinate transformation designed by the standard backstepping approach and the definition of consensus error, the following consensus tracking error and coordinate transformation are defined for the high-order MIMO nonlinear MAS (1):

$$\boldsymbol{z}_i^1=\sum_{j\in N}a_{ij}(\boldsymbol{x}_i^1-\boldsymbol{x}_j^1)+h_i(\boldsymbol{x}_i^1-\boldsymbol{y}^{\mathrm{r}}),\tag{2}$$

$$\boldsymbol{z}_i^q=\boldsymbol{x}_i^q-\bar{\boldsymbol{\alpha}}_i^{q-1},\tag{3}$$

$$\boldsymbol{z}_i^n=\boldsymbol{x}_i^n-\bar{\boldsymbol{\alpha}}_i^{n-1},\tag{4}$$

where $\bar{\boldsymbol{\alpha}}_i^{q-1}$ is the output of the following first-order filter. For instance,

$$\left.\begin{aligned}&\boldsymbol{\Gamma}_i^q\dot{\bar{\boldsymbol{\alpha}}}_i^q+\bar{\boldsymbol{\alpha}}_i^q=\boldsymbol{\alpha}_i^q,\quad \bar{\boldsymbol{\alpha}}_i^q(0)=\boldsymbol{\alpha}_i^q(0),\\&q=2,3,\cdots,n-1,\end{aligned}\right.\tag{5}$$

where, $\boldsymbol{\Gamma}_i^q=\mathrm{diag}(\tau_{i1}^q,\tau_{i2}^q,\cdots,\tau_{im}^q)$, $\tau_{il}^q>0$ is the time constant of the filter, and $\boldsymbol{\alpha}_i^q$ is the virtual control law of the qth subsystem of the ith agent, whose specific form will be given later. The first-order filter defined in Eq. (5) is the idea of DSC and addresses the "computational explosion" problem.

To facilitate the subsequent controller design and stability analysis, the following lemma is first given.

Lemma 2 Define $\tilde{\boldsymbol{L}}=\boldsymbol{L}+\boldsymbol{H}\in\mathbf{R}^{N\times N}$ and $\boldsymbol{\mathcal{L}}(\cdot)=\cdot\otimes\boldsymbol{I}_m$, where $\otimes$ is the Kronecker product and $\boldsymbol{I}_m$ is the $m\times m$ identity matrix; then, the augmented matrix $\boldsymbol{\mathcal{L}}(\tilde{\boldsymbol{L}})\in\mathbf{R}^{Nm\times Nm}$ is positive definite and satisfies:

$$\frac{1}{2}\boldsymbol{X}^{1\mathrm{T}}\boldsymbol{\mathcal{L}}(\tilde{\boldsymbol{L}})\boldsymbol{X}^1=\frac{1}{2}(\boldsymbol{Z}^1+\boldsymbol{\varpi})^{\mathrm{T}}\boldsymbol{\Delta}(\boldsymbol{Z}^1+\boldsymbol{\varpi})=\frac{1}{2}(\boldsymbol{Z}^1+\boldsymbol{\varpi})^{\mathrm{T}}\boldsymbol{X}^1, \tag{6}$$

where, $\boldsymbol{X}^1=[\boldsymbol{x}_1^1\ \ \boldsymbol{x}_2^1\ \ \cdots\ \ \boldsymbol{x}_N^1]^{\mathrm{T}}\in\mathbf{R}^{Nm}$; $\boldsymbol{z}_i^1=[z_{i1}^1\ \ z_{i2}^1\ \ \cdots\ \ z_{im}^1]^{\mathrm{T}}\in\mathbf{R}^m$, $\boldsymbol{Z}^1=[\boldsymbol{z}_1^1\ \ \boldsymbol{z}_2^1\ \ \cdots\ \ \boldsymbol{z}_N^1]^{\mathrm{T}}\in\mathbf{R}^{Nm}$; $\boldsymbol{\varpi}_i=[h_iy_1^{\mathrm{r}}\ \ h_iy_2^{\mathrm{r}}\ \ \cdots\ \ h_iy_m^{\mathrm{r}}]^{\mathrm{T}}$, $\boldsymbol{\varpi}=[\boldsymbol{\varpi}_1\ \ \boldsymbol{\varpi}_2\ \ \cdots\ \ \boldsymbol{\varpi}_N]^{\mathrm{T}}$; $z_{il}^1=\sum_{j\in N}a_{ij}(x_{il}^1-x_{jl}^1)+h_i(x_{il}^1-y_l^{\mathrm{r}})$, z_{il}^1, x_{il}^1 and y_l^{r} denote the lth component of the consensus tracking error vector $\boldsymbol{z}_i^1$, the state vector $\boldsymbol{x}_i^1$ and the virtual leader output vector $\boldsymbol{y}^{\mathrm{r}}$, respectively.

Proof see Appendix.

The design of a distributed cooperative anti-disturbance control protocol for higher order MIMO nonlinear MASs based on DSC and NDO will be given as follows:

Step 1 From Eq. (1), the first order subsystem of the ith agent can be described as

$$\dot{\boldsymbol{x}}_i^1=\boldsymbol{F}_i^1(\bar{\boldsymbol{x}}_i^1)+\boldsymbol{G}_i^1(\bar{\boldsymbol{x}}_i^1)\boldsymbol{x}_i^2+\boldsymbol{D}_i^1(\bar{\boldsymbol{x}}_i^1,t). \tag{7}$$

It follows from Eq. (2) that the consensus error of system (1) can be given as

$$\boldsymbol{z}_i^1=\sum_{j\in N}a_{ij}(\boldsymbol{x}_i^1-\boldsymbol{x}_j^1)+h_i(\boldsymbol{x}_i^1-\boldsymbol{y}^r). \tag{8}$$

To suppress the effect of the compound disturbance $\boldsymbol{D}_i^1$ on the performance of the closed-loop system, the following NDO is designed:

$$\hat{\boldsymbol{D}}_i^1=\boldsymbol{\eta}_i^1+\boldsymbol{P}_i^1, \tag{9}$$

$$\dot{\boldsymbol{\eta}}_i^1=-\boldsymbol{L}_i^1\boldsymbol{\eta}_i^1-\boldsymbol{L}_i^1(\boldsymbol{P}_i^1+\boldsymbol{F}_i^1+\boldsymbol{G}_i^1\boldsymbol{x}_i^2), \tag{10}$$

where $\boldsymbol{\eta}_i^1\in\mathbf{R}^m$ is the state vector of the disturbance observer, $\boldsymbol{P}_i^1\in\mathbf{R}^m$ is the designed function vector, and $\boldsymbol{L}_i^1=\partial\boldsymbol{P}_i^1/\partial\boldsymbol{x}_i^1\in\mathbf{R}^{m\times m}$.

Based on the output of the NDO, the following virtual control law can be designed for the first-order subsystem of the ith agent:

$$\left.\begin{aligned}&\boldsymbol{\alpha}_i^1=(-\boldsymbol{G}_i^1)^{-1}\left[\boldsymbol{C}_i^1(\boldsymbol{z}_i^1+\boldsymbol{\varpi}_i)+\boldsymbol{F}_i^1+\hat{\boldsymbol{D}}_i^1\right]\\&\lambda_{\min}(\boldsymbol{C}_i^1)\geqslant\frac{k_i}{2}\lambda_{\max}(\boldsymbol{\Delta})+\frac{1}{2}(\bar{\lambda}_i^1+1)\end{aligned}\right\}, \tag{11}$$

where $\boldsymbol{C}_i^1=(\boldsymbol{C}_i^1)^{\mathrm{T}}>0$ and $k_i>0$ are the parameters to be designed.

Step 2 From Eq. (2), the tracking error of the 2nd subsystem of the ith agent can be defined as

$$\boldsymbol{z}_i^2=\boldsymbol{x}_i^2-\bar{\boldsymbol{\alpha}}_i^1, \tag{12}$$

where $\bar{\boldsymbol{\alpha}}_i^1$ is the filtered signal of the virtual control law $\boldsymbol{\alpha}_i^1$ designed in the 1st step, and taking the derivative of both sides of Eq. (12) with respect to time yields

$$\dot{\boldsymbol{z}}_i^2=\boldsymbol{F}_i^2(\bar{\boldsymbol{x}}_i^2)+\boldsymbol{G}_i^2(\bar{\boldsymbol{x}}_i^2)\boldsymbol{x}_i^3+\boldsymbol{D}_i^2(\bar{\boldsymbol{x}}_i^2,t)-\dot{\bar{\boldsymbol{\alpha}}}_1^1. \tag{13}$$

Like Step 1, the following NDO is constructed for the 2nd subsystem of the ith agent to approximate the composite disturbance:

$$\hat{\boldsymbol{D}}_i^2=\boldsymbol{\eta}_i^2+\boldsymbol{P}_i^2, \tag{14}$$

$$\dot{\boldsymbol{\eta}}_i^2=-\boldsymbol{L}_i^2\boldsymbol{\eta}_i^2-\boldsymbol{L}_i^2(\boldsymbol{P}_i^2+\boldsymbol{F}_i^2+\boldsymbol{G}_i^2\boldsymbol{x}_i^3), \tag{15}$$

where $\boldsymbol{\eta}_i^2\in\mathbf{R}^m$ is the state vector of the disturbance observer, $\boldsymbol{P}_i^2\in\mathbf{R}^m$ is the designed function vector, and $\boldsymbol{L}_i^2=\partial\boldsymbol{P}_i^2/\partial\boldsymbol{x}_i^2\in\mathbf{R}^{m\times m}$.

Based on the output of the NDO, the following virtual control law can be designed for the 2nd subsystem of the ith agent:

$$\boldsymbol{\alpha}_i^2=(-\boldsymbol{G}_i^2)^{-1}[\boldsymbol{C}_i^2\boldsymbol{z}_i^2+(\boldsymbol{G}_i^1)^{\mathrm{T}}(\boldsymbol{z}_i^1+\boldsymbol{\varpi}_i)+\boldsymbol{F}_i^2-\dot{\bar{\boldsymbol{\alpha}}}_i^1+\hat{\boldsymbol{D}}_i^2], \tag{16}$$

where $\boldsymbol{C}_i^2=(\boldsymbol{C}_i^2)^{\mathrm{T}}>0$ is the parameter to be designed.

Step q $(3\leqslant q\leqslant n-1)$ It follows from Eq. (3) that the tracking error of the qth subsystem of the ith agent can be defined as

$$\boldsymbol{z}_i^q=\boldsymbol{x}_i^q-\bar{\boldsymbol{\alpha}}_i^{q-1}, \tag{17}$$

where $\bar{\boldsymbol{\alpha}}_i^{q-1}$ is the filtered signal of the virtual control law $\boldsymbol{\alpha}_i^{q-1}$ designed in the $(q-1)$th step, and taking the derivative of both sides of Eq. (17) with respect to time yields

$$\dot{\boldsymbol{z}}_i^q=\boldsymbol{F}_i^q(\bar{\boldsymbol{x}}_i^q)+\boldsymbol{G}_i^q(\bar{\boldsymbol{x}}_i^q)\boldsymbol{x}_i^{q+1}+\boldsymbol{D}_i^q(\bar{\boldsymbol{x}}_i^q,t)-\dot{\bar{\boldsymbol{\alpha}}}_1^{q-1}. \tag{18}$$

Like Step 1, the following NDO is constructed for the system to approximate the compound disturbance:

$$\hat{\boldsymbol{D}}_i^q=\boldsymbol{\eta}_i^q+\boldsymbol{P}_i^q, \tag{19}$$

$$\dot{\boldsymbol{\eta}}_i^q=-\boldsymbol{L}_i^q\boldsymbol{\eta}_i^q-\boldsymbol{L}_i^q(\boldsymbol{P}_i^q+\boldsymbol{F}_i^q+\boldsymbol{G}_i^q\boldsymbol{x}_i^{q+1}), \tag{20}$$

where $\boldsymbol{\eta}_i^q\in\mathbf{R}^m$ is the state vector of the disturbance observer, $\boldsymbol{P}_i^q\in\mathbf{R}^m$ is the designed function vector, and $\boldsymbol{L}_i^q=\partial\boldsymbol{P}_i^q/\partial\boldsymbol{x}_i^q\in\mathbf{R}^{m\times m}$.

Based on the output of the NDO, the following virtual control law can be designed for the qth subsystem of the ith agent:

$$\boldsymbol{\alpha}_i^q=(-\boldsymbol{G}_i^q)^{-1}[\boldsymbol{C}_i^q\boldsymbol{z}_i^q+(\boldsymbol{G}_i^{q-1})^{\mathrm{T}}\boldsymbol{z}_i^{q-1}+\boldsymbol{F}_i^q-\dot{\bar{\boldsymbol{\alpha}}}_i^{q-1}+\hat{\boldsymbol{D}}_i^q], \tag{21}$$

where $\boldsymbol{C}_i^q=(\boldsymbol{C}_i^q)^{\mathrm{T}}>0$ is the parameter to be designed.

Step n It follows from Eq. (4) that the tracking error of the nth subsystem of the ith agent can be defined as

$$\boldsymbol{z}_i^n=\boldsymbol{x}_i^n-\bar{\boldsymbol{\alpha}}_i^{n-1}, \tag{22}$$

where $\bar{\boldsymbol{\alpha}}_i^{n-1}$ is the filtered signal of the virtual control law $\boldsymbol{\alpha}_i^{n-1}$ designed in the $(n-1)$th step, and taking the derivative of both sides of Eq. (22) with respect to time yields

$$\dot{\boldsymbol{z}}_i^n = \boldsymbol{F}_i^n(\bar{\boldsymbol{x}}_i^n) + \boldsymbol{G}_i^n(\bar{\boldsymbol{x}}_i^n)\boldsymbol{u}_i + \boldsymbol{D}_i^n(\bar{\boldsymbol{x}}_i^n, t) - \dot{\bar{\boldsymbol{\alpha}}}_1^{n-1}. \quad (23)$$

Like Step 1, the following NDO is constructed for the system to approximate the compound disturbance:

$$\hat{\boldsymbol{D}}_i^n = \boldsymbol{\eta}_i^n + \boldsymbol{P}_i^n, \quad (24)$$

$$\dot{\boldsymbol{\eta}}_i^n = -\boldsymbol{L}_i^n\boldsymbol{\eta}_i^n - \boldsymbol{L}_i^n(\boldsymbol{P}_i^n + \boldsymbol{F}_i^n + \boldsymbol{G}_i^n\boldsymbol{u}), \quad (25)$$

where $\boldsymbol{\eta}_i^n \in \mathbf{R}^m$ is the state vector of the disturbance observer, $\boldsymbol{P}_i^n \in \mathbf{R}^m$ is the designed function vector, and $\boldsymbol{L}_i^n = \partial \boldsymbol{P}_i^n / \partial \boldsymbol{x}_i^n \in \mathbf{R}^{m\times m}$.

Based on the output of the NDO, the following control protocol can be designed for the ith agent

$$\begin{aligned}\boldsymbol{u}_i = &-\boldsymbol{G}_i^n(\boldsymbol{G}_i^n(\boldsymbol{G}_i^n)^{\mathrm{T}})^{-1}[\boldsymbol{C}_i^n\boldsymbol{z}_i^n + (\boldsymbol{G}_i^{n-1})^{\mathrm{T}}\boldsymbol{z}_i^{n-1} + \\ &\boldsymbol{F}_i^n - \dot{\bar{\boldsymbol{\alpha}}}_i^{n-1} + \hat{\boldsymbol{D}}_i^n],\end{aligned} \quad (26)$$

where $\boldsymbol{C}_i^n = (\boldsymbol{C}_i^n)^{\mathrm{T}} > 0$ is the parameter to be designed.

Theorem 1 Consider the high-order MIMO nonlinear MAS (1) satisfying Assumptions 1—3. The NDOs are given as Eqs. (18), (19), (23), (24), (28), (29), (33) and (34), and the virtual control laws are designed as Eqs. (11), (16) and (21). Under the NDO-based distributed cooperative anti-disturbance controller (26), the closed-loop system satisfies: output signal $\boldsymbol{y}_i$ is located in a small neighborhood of $\boldsymbol{y}^{\mathrm{r}}$ which is the output signal of the virtual leader, and all signals in the closed-loop system are bounded.

Proof Define the approximation error of NDO as follows:

$$\tilde{\boldsymbol{D}}_i^q = \boldsymbol{D}_i^q - \hat{\boldsymbol{D}}_i^q, \quad q = 1, 2, \cdots, n. \quad (27)$$

Differentiating Eq. (27) and invoking Eqs. (24) and (25) yields

$$\begin{aligned}\dot{\tilde{\boldsymbol{D}}}_i^q = &\dot{\boldsymbol{D}}_i^q - \dot{\boldsymbol{\eta}}_i^q - \boldsymbol{L}_i^q\dot{\boldsymbol{x}}_i^q = \\ &\dot{\boldsymbol{D}}_i^q + \boldsymbol{L}_i^q\boldsymbol{\eta}_i^q + \boldsymbol{L}_i^q\boldsymbol{P}_i^q - \boldsymbol{L}_i^q\boldsymbol{D}_i^q = \\ &\dot{\boldsymbol{D}}_i^q - \boldsymbol{L}_i^q\tilde{\boldsymbol{D}}_i^q.\end{aligned} \quad (28)$$

Define the filtering error of a first-order filter as

$$\boldsymbol{\varepsilon}_i^q = \bar{\boldsymbol{\alpha}}_i^q - \boldsymbol{\alpha}_i^q, \quad q = 1, 2, \cdots, n-1. \quad (29)$$

Differentiating both sides of Eq. (29) with respect to time t yields

$$\begin{aligned}\dot{\boldsymbol{\varepsilon}}_i^q = &-(\boldsymbol{\Gamma}_i^q)^{-1}\boldsymbol{\varepsilon}_i^q + \\ &\Big(-\frac{\partial\boldsymbol{\alpha}_i^q}{\partial\boldsymbol{x}_i^q}\dot{\boldsymbol{x}}_i^q - \frac{\partial\boldsymbol{\alpha}_i^q}{\partial\boldsymbol{z}_i^q}\dot{\boldsymbol{z}}_i^q - \frac{\partial\boldsymbol{\alpha}_i^q}{\partial\boldsymbol{\eta}_i^q}\dot{\boldsymbol{\eta}}_i^q + \ddot{\boldsymbol{y}}^{\mathrm{r}}\Big) = \\ &-(\boldsymbol{\Gamma}_i^q)^{-1}\boldsymbol{\varepsilon}_i^q + \boldsymbol{B}_i^q(\dot{\boldsymbol{z}}_i^q, \boldsymbol{z}_i^{q+1}, \boldsymbol{\varepsilon}_i^q, \boldsymbol{\eta}_i^q, \boldsymbol{y}^{\mathrm{r}}, \dot{\boldsymbol{y}}^{\mathrm{r}}, \ddot{\boldsymbol{y}}^{\mathrm{r}}),\end{aligned} \quad (30)$$

where $\boldsymbol{B}_i^q(\cdot)$ is a continuous function with respect to the variables $(\dot{\boldsymbol{z}}_i^q, \boldsymbol{z}_i^{q+1}, \boldsymbol{\varepsilon}_i^q, \boldsymbol{\eta}_i^q, \boldsymbol{y}^{\mathrm{r}}, \dot{\boldsymbol{y}}^{\mathrm{r}}, \ddot{\boldsymbol{y}}^{\mathrm{r}})$. Since the sets $\Pi_0 \in \mathbf{R}^{3m}$ and $\Pi_1 \in \mathbf{R}^{2m+1}$ are compact, $\Pi_0 \times \Pi_1$ is also compact. By the continuity of the function[49], the maximum value $\bar{\boldsymbol{B}}_i^q$ of function $\boldsymbol{B}_i^q(\cdot)$ exists on $\Pi_0 \times \Pi_1$. Therefore,

$$\dot{\boldsymbol{\varepsilon}}_i^q \leqslant -(\boldsymbol{\Gamma}_i^q)^{-1}\boldsymbol{\varepsilon}_i^q + \bar{\boldsymbol{B}}_i^q. \quad (31)$$

The candidate Lyapunov function is chosen as

$$\begin{aligned}V = &\frac{1}{2}(\boldsymbol{X}^1)^{\mathrm{T}}\boldsymbol{\mathcal{L}}(\tilde{\boldsymbol{L}})\boldsymbol{X}^1 + \sum_{i=1}^N\Big[\sum_{q=2}^n\frac{1}{2}(\boldsymbol{z}_i^q)^{\mathrm{T}}\boldsymbol{z}_i^q + \\ &\sum_{q=1}^{n-1}\frac{1}{2}(\boldsymbol{\varepsilon}_i^q)^{\mathrm{T}}\boldsymbol{\varepsilon}_i^q + \sum_{q=1}^n\frac{1}{2}(\tilde{\boldsymbol{D}}_i^q)^{\mathrm{T}}\tilde{\boldsymbol{D}}_i^q\Big].\end{aligned} \quad (32)$$

Remark In this paper, coupled relationships among Laplace matrix, leader-following adjacency matrix and consensus error are analyzed on the basis of Ref. [43] and summarized in Lemma 2. The study is on higher-order MIMO nonlinear MASs, which is more general in engineering practice. In addition, designed virtual control law is comparatively simple in structure compared with Ref. [43].

Differentiating Eq. (32) and combining Eq. (6) yields

$$\begin{aligned}\dot{V} = &(\boldsymbol{Z}^1 + \boldsymbol{\varpi})^{\mathrm{T}}\dot{\boldsymbol{X}}^1 + \sum_{i=1}^N\Big[\sum_{q=2}^n(\boldsymbol{z}_i^q)^{\mathrm{T}}\dot{\boldsymbol{z}}_i^q + \\ &\sum_{q=1}^{n-1}(\boldsymbol{\varepsilon}_i^q)^{\mathrm{T}}\dot{\boldsymbol{\varepsilon}}_i^q + \sum_{q=1}^n(\tilde{\boldsymbol{D}}_i^q)^{\mathrm{T}}\dot{\tilde{\boldsymbol{D}}}_i^q\Big],\end{aligned} \quad (33)$$

where

$$\begin{aligned}(\boldsymbol{Z}^1 + \boldsymbol{\varpi})^{\mathrm{T}}\dot{\boldsymbol{X}}^1 = &\sum_{l=1}^m(z_{1l}^1 + h_{1l}y_{1l}^{\mathrm{r}})\dot{x}_{1l}^1 + \\ &\sum_{l=1}^m(z_{2l}^1 + h_{2l}y_{2l}^{\mathrm{r}})\dot{x}_{2l}^1 + \cdots + \\ &\sum_{l=1}^m(z_{Nl}^1 + h_{Nl}y_{Nl}^{\mathrm{r}})\dot{x}_{Nl}^1 = \\ &\sum_{i=1}^N(\boldsymbol{z}_i^1 + \boldsymbol{\varpi}_i)^{\mathrm{T}}\dot{\boldsymbol{x}}_i^1.\end{aligned} \quad (34)$$

From Eq. (34), combining Eqs. (9), (10), (11), (14), (15), (19), (20), (24), (25), (29) and (31) yields

$$\begin{aligned}&\sum_{i=1}^N(\boldsymbol{z}_i^1 + \boldsymbol{\varpi}_i)^{\mathrm{T}}\dot{\boldsymbol{x}}_i^1 \leqslant \\ &\sum_{i=1}^N\Big\{-\Big[\lambda_{\min}(\boldsymbol{C}_i^1) - \frac{1}{2}(\bar{\lambda}_i^1 + 1)\Big](\boldsymbol{z}_i^1 + \boldsymbol{\varpi}_i)^{\mathrm{T}}(\boldsymbol{z}_i^1 + \boldsymbol{\varpi}_i) + \\ &(\boldsymbol{z}_i^1 + \boldsymbol{\varpi}_i)^{\mathrm{T}}\boldsymbol{G}_i^1\boldsymbol{z}_i^2 + \frac{1}{2}(\boldsymbol{\varepsilon}_i^1)^{\mathrm{T}}\boldsymbol{\varepsilon}_i^1 + \frac{1}{2}(\tilde{\boldsymbol{D}}_i^1)^{\mathrm{T}}\tilde{\boldsymbol{D}}_i^1\Big\} \leqslant\end{aligned}$$

$$\sum_{i=1}^{N}\Big[-\frac{k}{2}\lambda_{\max}(\boldsymbol{\Delta})(\boldsymbol{z}_i^1+\boldsymbol{\varpi}_i)^{\mathrm{T}}(\boldsymbol{z}_i^1+\boldsymbol{\varpi}_i)+$$
$$(\boldsymbol{z}_i^1+\boldsymbol{\varpi}_i)^{\mathrm{T}}\boldsymbol{G}_i^1\boldsymbol{z}_i^2+\frac{1}{2}(\boldsymbol{\varepsilon}_i^1)^{\mathrm{T}}\boldsymbol{\varepsilon}_i^1+\frac{1}{2}(\tilde{\boldsymbol{D}}_i^1)^{\mathrm{T}}\tilde{\boldsymbol{D}}_i^1\Big]\leqslant$$
$$-\frac{k}{2}(\boldsymbol{X}^1)^{\mathrm{T}}\boldsymbol{\mathcal{L}}(\tilde{\boldsymbol{L}})\boldsymbol{X}^1+\sum_{i=1}^{N}\Big[(\boldsymbol{z}_i^1+\boldsymbol{\varpi}_i)^{\mathrm{T}}\boldsymbol{G}_i^1\boldsymbol{z}_i^2+$$
$$\frac{1}{2}(\boldsymbol{\varepsilon}_i^1)^{\mathrm{T}}\boldsymbol{\varepsilon}_i^1+\frac{1}{2}(\tilde{\boldsymbol{D}}_i^1)^{\mathrm{T}}\tilde{\boldsymbol{D}}_i^1\Big],\tag{35}$$

$$\sum_{q=2}^{n}(\boldsymbol{z}_i^q)^{\mathrm{T}}\dot{\boldsymbol{z}}_i^q=\sum_{q=2}^{n}\Big[-(\boldsymbol{z}_i^q)^{\mathrm{T}}\boldsymbol{C}_i^q\boldsymbol{z}_i^q+(\boldsymbol{z}_i^q)^{\mathrm{T}}\tilde{\boldsymbol{D}}_i^q\Big]+$$
$$\sum_{q=2}^{n-1}(\boldsymbol{z}_i^q)^{\mathrm{T}}\boldsymbol{G}_i^q\boldsymbol{\varepsilon}_i^q-(\boldsymbol{z}_i^2)^{\mathrm{T}}\boldsymbol{G}_i^1(\boldsymbol{z}_i^1+\boldsymbol{\varpi}_i),\tag{36}$$

$$(\boldsymbol{\varepsilon}_i^q)^{\mathrm{T}}\dot{\boldsymbol{\varepsilon}}_i^q\leqslant-(\boldsymbol{\varepsilon}_i^q)^{\mathrm{T}}(\boldsymbol{\Gamma}_i^q)^{-1}\boldsymbol{\varepsilon}_i^q$$
$$+\frac{1}{2}(\boldsymbol{\varepsilon}_i^q)^{\mathrm{T}}\boldsymbol{\varepsilon}_i^q+\frac{1}{2}(\bar{\boldsymbol{B}}_i^q)^{\mathrm{T}}\bar{\boldsymbol{B}}_i^q,\tag{37}$$

$$(\tilde{\boldsymbol{D}}_i^q)^{\mathrm{T}}\dot{\tilde{\boldsymbol{D}}}_i^q\leqslant-(\tilde{\boldsymbol{D}}_i^q)^{\mathrm{T}}\boldsymbol{L}_i^q\tilde{\boldsymbol{D}}_i^q+\frac{1}{2}(\tilde{\boldsymbol{D}}_i^q)^{\mathrm{T}}\tilde{\boldsymbol{D}}_i^q+\frac{1}{2}(\beta_i^q)^2\leqslant$$
$$-\Big[\lambda_{\min}(\boldsymbol{L}_i^q)-\frac{1}{2}\Big](\tilde{\boldsymbol{D}}_i^q)^{\mathrm{T}}\tilde{\boldsymbol{D}}_i^q+\frac{1}{2}(\beta_i^q)^2.\tag{38}$$

Substituting Eqs. (34)—(38) into Eq. (33) yields

$$\dot{V}\leqslant\sum_{i=1}^{N}(\boldsymbol{z}_i^1+\boldsymbol{\varpi}_i)^{\mathrm{T}}\dot{\boldsymbol{x}}_i^1+$$
$$\sum_{i=1}^{N}\Big[\sum_{q=2}^{n}(\boldsymbol{z}_i^q)^{\mathrm{T}}\dot{\boldsymbol{z}}_i^q+\sum_{q=1}^{n-1}(\boldsymbol{\varepsilon}_i^q)^{\mathrm{T}}\dot{\boldsymbol{\varepsilon}}_i^q+\sum_{q=1}^{n}(\tilde{\boldsymbol{D}}_i^q)^{\mathrm{T}}\dot{\tilde{\boldsymbol{D}}}_i^q\Big]\leqslant$$
$$-\frac{k}{2}(\boldsymbol{X}^1)^{\mathrm{T}}\boldsymbol{\mathcal{L}}(\tilde{\boldsymbol{L}})\boldsymbol{X}^1-$$
$$\sum_{i=1}^{N}\Big[\sum_{q=2}^{n-1}\Big(\lambda_{\min}(\boldsymbol{C}_i^q)-\frac{1}{2}(\bar{\lambda}_i^q+1)\Big)(\boldsymbol{z}_i^q)^{\mathrm{T}}\boldsymbol{z}_i^q+$$
$$\Big(\lambda_{\min}(\boldsymbol{C}_i^n)-\frac{1}{2}\Big)(\boldsymbol{z}_i^n)^{\mathrm{T}}\boldsymbol{z}_i^n\Big]-$$
$$\sum_{i=1}^{N}\Big[\sum_{q=1}^{n-1}(\lambda_{\min}(\boldsymbol{\Gamma}_i^q)^{-1}-1)(\boldsymbol{\varepsilon}_i^q)^{\mathrm{T}}\boldsymbol{\varepsilon}_i^q\Big]-$$
$$\sum_{i=1}^{N}\Big[\sum_{q=1}^{n}(\lambda_{\min}(\boldsymbol{L}_i^q)-1)(\tilde{\boldsymbol{D}}_i^q)^{\mathrm{T}}\tilde{\boldsymbol{D}}_i^q\Big]+$$
$$\sum_{i=1}^{N}\Big(\sum_{q=1}^{n-1}\frac{1}{2}(\bar{\boldsymbol{B}}_i^q)^{\mathrm{T}}\bar{\boldsymbol{B}}_i^q+\sum_{q=1}^{n}\frac{1}{2}(\beta_i^q)^2\Big)\leqslant$$
$$-\kappa V+M,\tag{39}$$

where

$$\kappa=\min\Big\{k,\lambda_{\min}(\boldsymbol{C}_i^q)-\frac{1}{2}(\bar{\lambda}_i^q+1),$$
$$\lambda_{\min}(\boldsymbol{C}_i^n)-\frac{1}{2},\lambda_{\min}(\boldsymbol{\Gamma}_i^q)^{-1}-1,$$
$$\lambda_{\min}(\boldsymbol{L}_i^q)-1\Big\}>0,$$

$$M=\sum_{i=1}^{N}\Big[\sum_{q=1}^{n-1}\frac{1}{2}(\bar{\boldsymbol{B}}_i^q)^{\mathrm{T}}\bar{\boldsymbol{B}}_i^q+\sum_{q=1}^{n}\frac{1}{2}(\beta_i^q)^2\Big],$$
$$q=1,2,\cdots,n.$$

This concludes the proof.

3 Simulation Results

In this section, simulations are performed to verify the effectiveness of the proposed distributed anti-disturbance cooperative control protocol. The MASs consist of one virtual leader 0 and four followers with numbered A1, A2, A3 and A4. The output of the virtual leader is $\boldsymbol{y}^{\mathrm{r}}=[\sin 0.5t\quad\cos 0.5t]^{\mathrm{T}}$, and the topology is shown in Fig. 1. The corresponding degree matrix $\boldsymbol{B}$, adjacency weight matrix $\boldsymbol{A}$ and Laplace matrix are given previously. $\boldsymbol{H}=\mathrm{diag}(0,1,0,0)$, $\boldsymbol{\mathcal{L}}(\tilde{\boldsymbol{L}})=\boldsymbol{\mathcal{L}}(\boldsymbol{L}+\boldsymbol{H})=\boldsymbol{\mathcal{L}}(\boldsymbol{L})+\boldsymbol{\mathcal{L}}(\boldsymbol{H})$, and $\lambda_{\max}(\boldsymbol{\Delta})=4.414$. The dynamical system model of each follower is described as

$$\dot{\boldsymbol{x}}_i^1=\begin{bmatrix}x_{i1}^1\sin x_{i1}^1\\x_{i2}^1\end{bmatrix}+\begin{bmatrix}x_{i1}^2\\x_{i2}^2\end{bmatrix}+\boldsymbol{D}_i^1,$$
$$\dot{\boldsymbol{x}}_i^2=\begin{bmatrix}0.1x_{i1}^1x_{i1}^2/x_{11}^1+1\\x_{i2}^2\cos x_{i1}^1\sin x_{i1}^2\end{bmatrix}+\begin{bmatrix}u_1\\u_2\end{bmatrix}+\boldsymbol{D}_i^2,$$
$$\boldsymbol{y}=\boldsymbol{x}_i^1,\quad i=1,2,3,4.$$

The initial values for each follower are $\boldsymbol{x}_{1,0}=[0.4\quad0\quad0.3\quad0]^{\mathrm{T}}$, $\boldsymbol{x}_{2,0}=[0.3\quad0.2\quad0\quad0]^{\mathrm{T}}$, $\boldsymbol{x}_{3,0}=[0.3\quad0.2\quad0.5\quad0]^{\mathrm{T}}$ and $\boldsymbol{x}_{4,0}=[0.3\quad0.2\quad0.2\quad0]^{\mathrm{T}}$, the parameter k_i is chosen to be $k_i=2$, and the other parameters and controller design parameters are shown in Table 1. From the parameters in Table 1, the parameter $\boldsymbol{C}_i^1$ satisfies the conditions of Eq. (11).

Simulation results show the performance of the proposed distributed anti-disturbance cooperative control protocol in Figs. 2—7. Figures 2—4 show the tracking effect $\boldsymbol{x}_i^1$, tracking error $\boldsymbol{e}^{T_i}$, and consensus error $\boldsymbol{z}_i^1$, respectively. The tracking error is used to describe

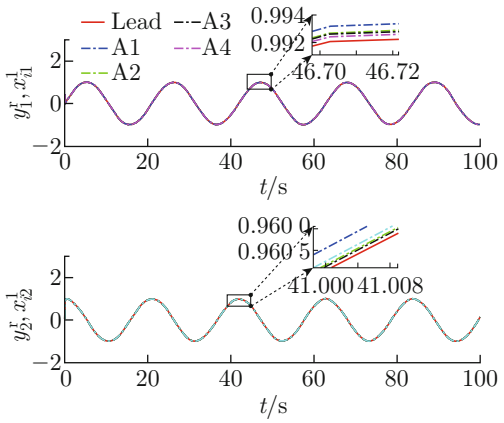

Fig. 2 Tracking effect of followers

Table 1 Other parameters and controller design parameters

Agent	A1	A2	A3	A4
$\boldsymbol{D}^1$	$D_{11}^1=0.3\cos(0.5t)$ $D_{12}^1=0.1\cos(0.3t)$	$D_{21}^1=0.7\sin(0.1t)$ $D_{22}^1=0.5\sin(0.1t)$	$D_{31}^1=0.2\sin(0.2t)$ $D_{32}^1=0.5\sin(0.1t)$	$D_{41}^1=0.6\cos(0.3t)$ $D_{41}^1=0.2\cos(0.2t)$
$\boldsymbol{C}_i^1$	$\begin{bmatrix}100 & 0\\ 0 & 100\end{bmatrix}$	$\begin{bmatrix}100 & 0\\ 0 & 100\end{bmatrix}$	$\begin{bmatrix}100 & 0\\ 0 & 100\end{bmatrix}$	$\begin{bmatrix}100 & 0\\ 0 & 100\end{bmatrix}$
$\boldsymbol{P}_i^1$	$\begin{bmatrix}0.8x_{11}^1+0.3\\ 0.8x_{12}^1+0.1\end{bmatrix}$	$\begin{bmatrix}x_{21}^1\\ x_{22}^1\end{bmatrix}$	$\begin{bmatrix}x_{31}^1\\ x_{32}^1\end{bmatrix}$	$\begin{bmatrix}x_{41}^1+0.3\\ x_{42}^1\end{bmatrix}$
$\boldsymbol{D}^2$	$D_{11}^2=0.8\sin(0.5t)$ $D_{12}^2=0.1\cos(0.2t)$	$D_{21}^2=0.6\sin(0.5t)$ $D_{22}^2=0.5\cos(0.2t)$	$D_{31}^2=0.5\sin(0.2t)$ $D_{32}^2=0.3\cos(0.2t)$	$D_{41}^2=0.6\sin(0.7t)$ $D_{42}^2=0.3\cos(0.3t)$
$\boldsymbol{C}_i^2$	$\begin{bmatrix}10 & 0\\ 0 & 10\end{bmatrix}$	$\begin{bmatrix}10 & 0\\ 0 & 10\end{bmatrix}$	$\begin{bmatrix}10 & 0\\ 0 & 10\end{bmatrix}$	$\begin{bmatrix}10 & 0\\ 0 & 10\end{bmatrix}$
$\boldsymbol{P}_i^2$	$[0.8x_{11}^2 \quad 0.8x_{12}^2]^{\mathrm{T}}$	$[x_{21}^2 \quad x_{22}^2]^{\mathrm{T}}$	$[x_{31}^2 \quad x_{32}^2]^{\mathrm{T}}$	$[x_{41}^2 \quad x_{42}^2]^{\mathrm{T}}$

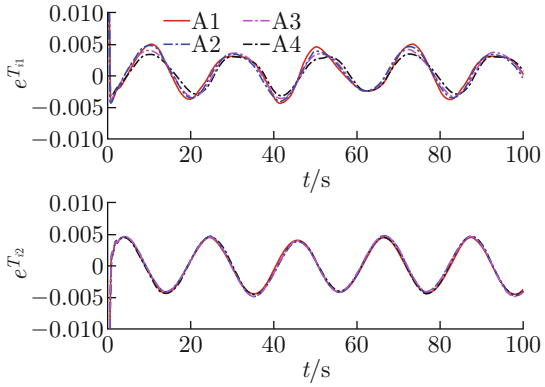

Fig. 3 Tracking error of followers to leaders

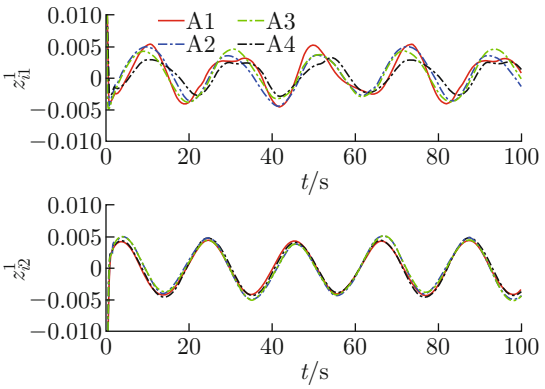

Fig. 4 Consensus error of followers

the tracking performance of the follower i output signal $\boldsymbol{x}_i$ on the virtual leader 0 output signal $\boldsymbol{y}^{\mathrm{r}}$, that is, $\lim\limits_{t\to\infty}\left\|\boldsymbol{x}_i^1-\boldsymbol{y}^{\mathrm{r}}\right\|=0$. The consensus error is used to describe the deviation of the states among agents, and the smaller its value, the better MASs can work cooperatively, that is, $\lim\limits_{t\to\infty}\sum\limits_{j\in N}a_{ij}(\boldsymbol{x}_i^1-\boldsymbol{x}_j^1)+h_i(\boldsymbol{x}_i^1-\boldsymbol{y}^{\mathrm{r}})=0$.

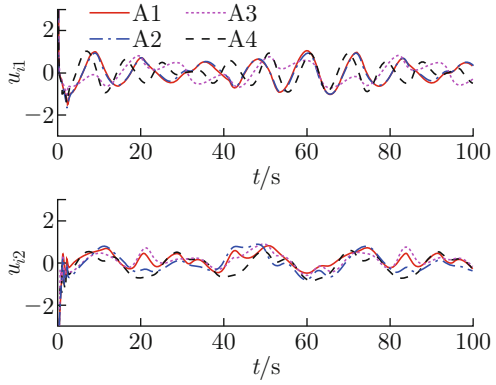

Fig. 5 Control input of followers

From Figs. 3 and 4, it can be seen that after about 3 s of adjustment, the tracking error and consensus error of all followers are stable within ±1%, which means that the designed controller has a good control effect. Figure 5 shows the controller input signals (u_{i1} and u_{i2}), because the initial state of each agent is different and needs to be adjusted quickly, so input signals are jittered at the beginning, after which the signals are stable within ±2. From Fig. 6, it can be seen that the designed NDO is effective for online estimation of compound disturbances. To further analyze the effect of NDO on the performance of the closed-loop system, the simulation comparison plots of the follower consensus error and tracking error with and without the addition of NDO are given in Fig. 7. It can be seen that the addition of NDO can reduce the tracking error and consistency error by about five times at the peak.

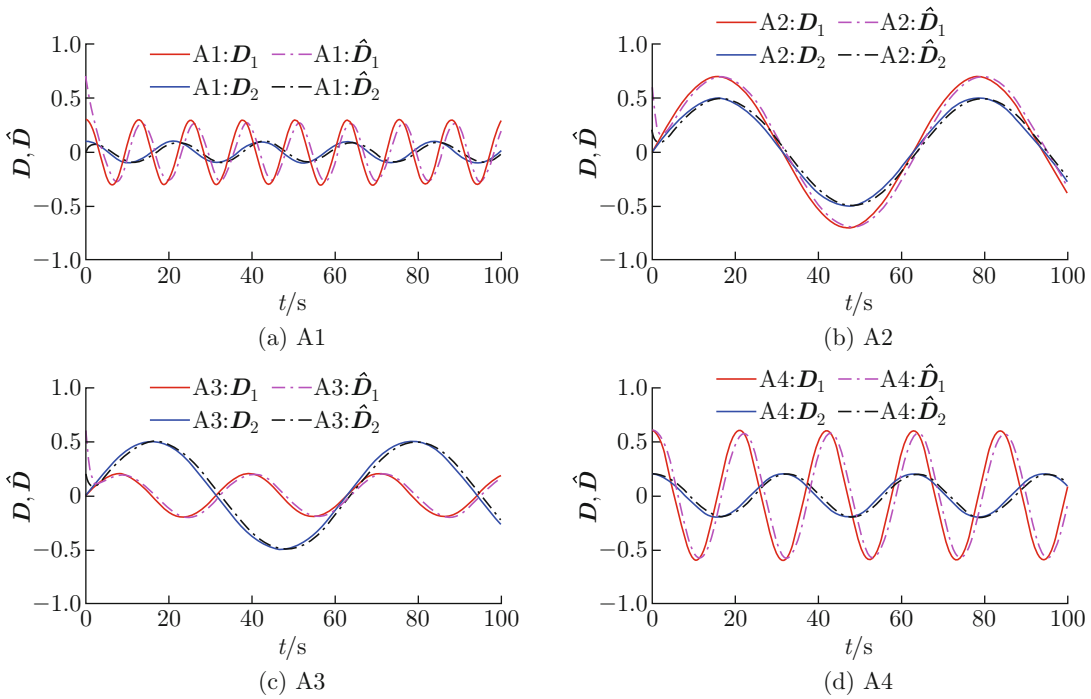

(a) A1 (b) A2 (c) A3 (d) A4

Fig. 6 Estimated and actual values of disturbances

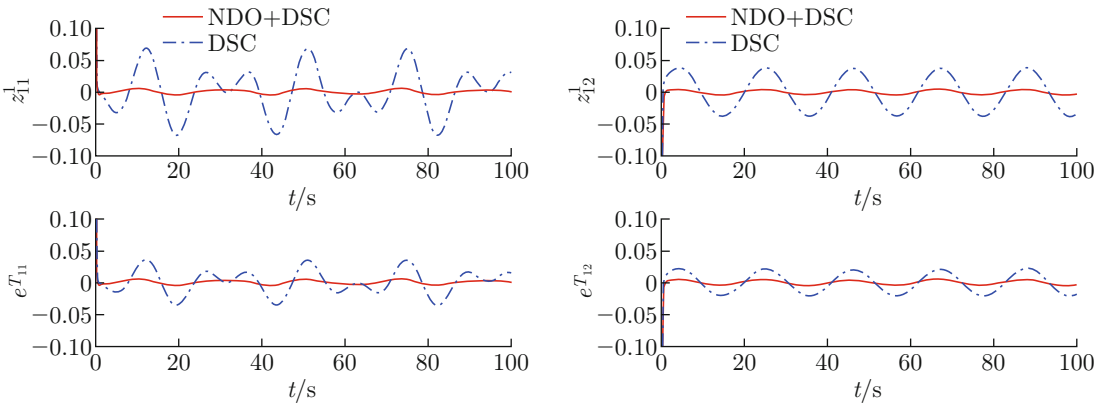

(a) A1 state 1 (b) A1 state 2

Fig. 7 Comparative consensus and tracking errors analysis of A1 with or without NDO

4 Conclusion

In this paper, the leader-following consensus problem is investigated for a class of high-order MIMO nonlinear MASs with uncertainties and dynamic disturbances in undirected topology. By employing NDO to estimate the compound disturbances online and based on DSC, a distributed cooperative anti-disturbance control protocol is designed for the high-order MIMO nonlinear MASs. By analyzing the coupled relationships among Laplace matrix, leader-following adjacency matrix and consensus error, the Lyapunov function is constructed to ensure that the designed control protocol is structurally simple and all signals in the closed loop system are bounded. In the future, the distributed anti-disturbance cooperative control protocol for high-order MIMO nonlinear MASs will be considered in the presence of directed graphs, dynamic topologies and practical engineering application.

Conflict of Interest The authors declare that they have no conflict of interest.

References

[1] ZHANG X, CHEN M Y, WANG L, et al. Fault-tolerant consensus for a network of multi-agent systems with actuator faults [J]. *Journal of Shanghai Jiao Tong University*, 2015, **49**(6): 806-811 (in Chinese).

[2] OH K K, PARK M C, AHN H S. A survey of

multi-agent formation control [J]. *Automatica*, 2015, **53**: 424-440.

[3] THUNBERG J, GONCALVES J, HU X M. Consensus and formation control on SE(3) for switching topologies [J]. *Automatica*, 2016, **66**: 109-121.

[4] DASGUPTA P. A multiagent swarming system for distributed automatic target recognition using unmanned aerial vehicles [J]. *IEEE Transactions on Systems, Man, and Cybernetics - Part A: Systems and Humans*, 2008, **38**(3): 549-563.

[5] SHI H, WANG L, CHU T G. Swarming behavior of multi-agent systems [J]. *Journal of Control Theory and Applications*, 2004, **2**(4): 313-318.

[6] QIN J H, FU W M, GAO H J, et al. Distributed k-means algorithm and fuzzy c-means algorithm for sensor networks based on multiagent consensus theory [J]. *IEEE Transactions on Cybernetics*, 2017, **47**(3): 772-783.

[7] LI X G, HU X Y, ZHANG R Q, et al. Routing protocol design for underwater optical wireless sensor networks: A multiagent reinforcement learning approach [J]. *IEEE Internet of Things Journal*, 2020, **7**(10): 9805-9818.

[8] PUTRA S A, TRILAKSONO B R, RIYANSYAH M, et al. Intelligent sensing in multiagent-based wireless sensor network for bridge condition monitoring system [J]. *IEEE Internet of Things Journal*, 2019, **6**(3): 5397-5410.

[9] YEUNG C S K, POON A S Y, WU F F. Game theoretical multi-agent modelling of coalition formation for multilateral trades [J]. *IEEE Transactions on Power Systems*, 1999, **14**(3): 929-934.

[10] LIN Z Y, WANG L L, HAN Z M, et al. Distributed formation control of multi-agent systems using complex Laplacian [J]. *IEEE Transactions on Automatic Control*, 2014, **59**(7): 1765-1777.

[11] QIU X F, ZHANG Y X, LI K Z. Successive lag cluster consensus on multi-agent systems via delay-dependent impulsive control [J]. *Chinese Physics B*, 2019, **28**(5): 050501.

[12] HONG Y G, HU J P, GAO L X. Tracking control for multi-agent consensus with an active leader and variable topology [J]. *Automatica*, 2006, **42**(7): 1177-1182.

[13] LIN P, JIA Y M. Multi-agent consensus with diverse time-delays and jointly-connected topologies [J]. *Automatica*, 2011, **47**(4): 848-856.

[14] REN W, BEARD R W. Consensus seeking in multiagent systems under dynamically changing interaction topologies [J]. *IEEE Transactions on Automatic Control*, 2005, **50**(5): 655-661.

[15] BLONDEL V D, HENDRICKX J M, TSITSIKLIS J N. On Krause's multi-agent consensus model with state-dependent connectivity [J]. *IEEE Transactions on Automatic Control*, 2009, **54**(11): 2586-2597.

[16] WANG F Y, YANG H Y, LIU Z X, et al. Containment control of leader-following multi-agent systems with jointly-connected topologies and time-varying delays [J]. *Neurocomputing*, 2017, **260**: 341-348.

[17] HONG Y G, CHEN G R, BUSHNELL L. Distributed observers design for leader-following control of multiagent networks [J]. *Automatica*, 2008, **44**(3): 846-850.

[18] LI X W, SUN Z Y, TANG Y, et al. Adaptive event-triggered consensus of multiagent systems on directed graphs [J]. *IEEE Transactions on Automatic Control*, 2021, **66**(4): 1670-1685.

[19] GARCIA E, CAO Y C, CASBEER D W. Decentralized event-triggered consensus with general linear dynamics [J]. *Automatica*, 2014, **50**(10): 2633-2640.

[20] YU M, YAN C, XIE D M, et al. Event-triggered tracking consensus with packet losses and time-varying delays [J]. *IEEE/CAA Journal of Automatica Sinica*, 2016, **3**(2): 165-173.

[21] BORGERS D P, HEEMELS W P M H. Event-separation properties of event-triggered control systems [J]. *IEEE Transactions on Automatic Control*, 2014, **59**(10): 2644-2656.

[22] WANG L, XIAO F. Finite-time consensus problems for networks of dynamic agents [J]. *IEEE Transactions on Automatic Control*, 2010, **55**(4): 950-955.

[23] LI S H, DU H B, LIN X Z. Finite-time consensus algorithm for multi-agent systems with double-integrator dynamics [J]. *Automatica*, 2011, **47**(8): 1706-1712.

[24] CAO Y C, REN W. Finite-time consensus for multiagent networks with unknown inherent nonlinear dynamics [J]. *Automatica*, 2014, **50**(10): 2648-2656.

[25] LIU X Y, LAM J, YU W W, et al. Finite-time consensus of multiagent systems with a switching protocol [J]. *IEEE Transactions on Neural Networks and Learning Systems*, 2016, **27**(4): 853-862.

[26] LI C Y, QU Z H. Distributed finite-time consensus of nonlinear systems under switching topologies [J]. *Automatica*, 2014, **50**(6): 1626-1631.

[27] ZOU W C, SHI P, XIANG Z R, et al. Finite-time consensus of second-order switched nonlinear multi-agent systems [J]. *IEEE Transactions on Neural Networks and Learning Systems*, 2020, **31**(5): 1757-1762.

[28] DU H B, WEN G H, WU D, et al. Distributed fixed-time consensus for nonlinear heterogeneous multiagent systems [J]. *Automatica*, 2020, **113**: 108797.

[29] HONG H F, YU W W, WEN G H, et al. Distributed robust fixed-time consensus for nonlinear and disturbed multiagent systems [J]. *IEEE Transactions on Systems, Man, and Cybernetics: Systems*, 2017, **47**(7): 1464-1473.

[30] HAN J, WANG C H, YI G X. Cooperative control of UAV based on multi-agent system [C]//*2013 IEEE 8th Conference on Industrial Electronics and Applications*. Melbourne: IEEE, 2013: 96-101.

[31] LIU B, ZHANG H T, WU Y, et al. Distributed consensus control of multi-USV systems [M]//International conference on intelligent robotics and applications. Cham: Springer, 2017: 628-635.

[32] GAO C, WANG Z D, HE X, et al. On consensus of second-order multiagent systems with actuator saturations: A generalized-nyquist-criterion-based approach [J]. *IEEE Transactions on Cybernetics*, 2022, **52**(9): 9048-9058.

[33] LIU T Q, LIU M Q, WEN G H, et al. Consensus of linear MIMO multiagent systems: Appointed-time reduced-order observer-based protocols [J]. *IEEE Transactions on Cybernetics*, 2022, **52**(10): 10604-10610.

[34] WU Z M, WU Y F, YUE D. Distributed adaptive neural consensus tracking control of MIMO stochastic nonlinear multiagent systems with actuator failures and unknown dead zones [J]. *International Journal of Adaptive Control and Signal Processing*, 2018, **32**(12): 1694-1714.

[35] AI X L, YU J Q, JIA Z Y, et al. Disturbance observer-based consensus tracking for nonlinear multiagent systems with switching topologies [J]. *International Journal of Robust and Nonlinear Control*, 2018, **28**(6): 2144-2160.

[36] YANG X W, DENG W X, YAO J Y. Disturbance-observer-based adaptive command filtered control for uncertain nonlinear systems [J]. *ISA Transactions*, 2022, **130**: 490-499.

[37] ZHANG H W, LEWIS F L. Adaptive cooperative tracking control of higher-order nonlinear systems with unknown dynamics [J]. *Automatica*, 2012, **48**(7): 1432-1439.

[38] ZHOU Y L, CHEN M, JIANG C S. Robust tracking control of uncertain MIMO nonlinear systems with application to UAVs [J]. *IEEE/CAA Journal of Automatica Sinica*, 2015, **2**(1): 25-32.

[39] TONG S C, LI Y M. Adaptive fuzzy output feedback control of MIMO nonlinear systems with unknown dead-zone inputs [J]. *IEEE Transactions on Fuzzy Systems*, 2013, **21**(1): 134-146.

[40] MADANI T, BENALLEGUE A. Adaptive control via backstepping technique and neural networks of a quadrotor helicopter [J]. *IFAC Proceedings Volumes*, 2008, **41**(2): 6513-6518.

[41] SWAROOP D, HEDRICK J K, YIP P P, et al. Dynamic surface control for a class of nonlinear systems [J]. *IEEE Transactions on Automatic Control*, 2000, **45**(10): 1893-1899.

[42] YANG X W, DENG W X, YAO J Y. Neural adaptive dynamic surface asymptotic tracking control of hydraulic manipulators with guaranteed transient performance [J]. *IEEE Transactions on Neural Networks and Learning Systems*, 2022. https://doi.org/10.1109/TNNLS.2022.3141463.

[43] ZHOU Q, CHEN G D, LU R Q, et al. Disturbance-observer-based event-triggered control for multi-agent systems with input saturation [J]. *Scientia Sinica* (*Informationis*), 2019, **49**(11): 1502-1516 (in Chinese).

[44] NGUYEN A T, XUAN-MUNG N, HONG S K. Quadcopter adaptive trajectory tracking control: A new approach via backstepping technique [J]. *Applied Sciences*, 2019, **9**(18): 3873.

[45] ZUO Z Y, TIAN B L, DEFOORT M, et al. Fixed-time consensus tracking for multiagent systems with high-order integrator dynamics [J]. *IEEE Transactions on Automatic Control*, 2018, **63**(2): 563-570.

[46] PU M, WU Q X, JIANG C S, et al. Application of adaptive second-order dynamic terminal sliding mode control to near space vehicle [J]. *Journal of Aerospace Power*, 2010, **25**(5): 1169-1176.

[47] CHEN M, JIANG B. Robust attitude control of near space vehicles with time-varying disturbances [J]. *International Journal of Control, Automation and Systems*, 2013, **11**(1): 182-187.

[48] TEE K P, GE S S. Control of fully actuated ocean surface vessels using a class of feedforward approximators [J]. *IEEE Transactions on Control Systems Technology*, 2006, **14**(4): 750-756.

[49] LI T S, ZHANG H Y, YANG X Y. DSC approach to robust adaptive fuzzy tracking control for strict-feedback nonlinear systems [C]//*2008 Fifth International Conference on Fuzzy Systems and Knowledge Discovery*. Jinan: IEEE, 2008: 70-74.

Appendix

From the definition of the augmented matrix $\boldsymbol{\mathcal{L}}(\cdot)$, the following equation holds:

$$\boldsymbol{\mathcal{L}}(\tilde{\boldsymbol{L}}) = \boldsymbol{\mathcal{L}}(\boldsymbol{L}+\boldsymbol{H}) = \boldsymbol{\mathcal{L}}(\boldsymbol{L}) + \boldsymbol{\mathcal{L}}(\boldsymbol{H}), \tag{A1}$$

where $\boldsymbol{\mathcal{L}}(\boldsymbol{L}) \in \mathbf{R}^{Nm\times Nm}$ and $\boldsymbol{\mathcal{L}}(\boldsymbol{H}) \in \mathbf{R}^{Nm\times Nm}$ are both real symmetric matrices. Since $\boldsymbol{\mathcal{L}}(\boldsymbol{H})$ is a diagonal matrix with main diagonal elements $h_i \geqslant 0$, $\boldsymbol{\mathcal{L}}(\boldsymbol{H})$ is semipositive definite.

Noting

$$\boldsymbol{\mathcal{L}}(\boldsymbol{L}) = \boldsymbol{\mathcal{L}}(\boldsymbol{B}-\boldsymbol{A}) = \begin{bmatrix} c_{11} & \cdots & c_{1Nm} \\ \vdots & & \vdots \\ c_{Nm1} & \cdots & c_{NmNm} \end{bmatrix}, \tag{A2}$$

let λ_0 be any eigenvalue of $\boldsymbol{\mathcal{L}}(\boldsymbol{L})$ and ξ_0 be the eigenvector associated with λ_0, such that $\boldsymbol{\mathcal{L}}(\boldsymbol{L})\xi_0 = \lambda_0\xi_0$. The ith component of ξ_0 is $\xi_i\,(i=1,2,\cdots,Nm)$, and $\boldsymbol{\mathcal{L}}(\boldsymbol{L})\xi_0 = \lambda_0\xi_0$ can be expressed as a system of linear equations as follows:

$$\left.\begin{aligned} c_{11}\xi_1 + c_{12}\xi_2 + \cdots + c_{1Nm}\xi_{Nm} &= \lambda_0\xi_1 \\ c_{21}\xi_1 + c_{22}\xi_2 + \cdots + c_{2Nm}\xi_{Nm} &= \lambda_0\xi_2 \\ \vdots & \\ c_{Nm1}\xi_1 + c_{Nm2}\xi_2 + \cdots + c_{NmNm}\xi_{Nm} &= \lambda_0\xi_{Nm} \end{aligned}\right\}. \tag{A3}$$

Suppose that $|\xi_r|$ is the largest of the magnitudes $|\xi_1|$, $|\xi_2|, \cdots, |\xi_{Nm}|$. Based on Eq. (A3), the following

formula holds:

$$(\lambda_0 - c_{rr})\xi_r = c_{r1}\xi_1 + \cdots + c_{r(r-1)}\xi_{r-1} + c_{r(r+1)}\xi_{r+1} + \cdots + c_{rNm}\xi_{Nm}, \tag{A4}$$

$$|(\lambda_0 - c_{rr})|\,|\xi_r| \leqslant |c_{r1}|\,|\xi_1| + \cdots + \left|c_{r(r-1)}\right|\,|\xi_{r-1}| + \left|c_{r(r+1)}\right|\,|\xi_{r+1}| + \cdots + |c_{rNm}|\,|\xi_{Nm}| \leqslant \left(|c_{r1}| + \cdots + \left|c_{r(r-1)}\right| + \left|c_{r(r+1)}\right| + \cdots + |c_{rNm}|\right)|\xi_r| \leqslant \hbar\,|\xi_r|\,, \tag{A5}$$

$$c_{rr} - \hbar \leqslant \lambda_0 \leqslant c_{rr} + \hbar, \tag{A6}$$

where $\hbar = |c_{r1}| + \cdots + \left|c_{r(r-1)}\right| + \left|c_{r(r+1)}\right| + \cdots + |c_{rNm}|$. From graph theory, it follows that

$$c_{rr} = -\left(c_{r1} + \cdots + c_{r(r-1)} + c_{r(\mathrm{r}+1)} + \cdots + c_{rNm}\right) = \hbar \geqslant 0. \tag{A7}$$

It follows from Eqs. (A6) and (A7) that any eigenvalue of $\boldsymbol{\mathcal{L}}(\boldsymbol{L})$ satisfies $\lambda_0 \geqslant 0$. Whereupon $\boldsymbol{\mathcal{L}}(\boldsymbol{L})$ is a semipositive definite real symmetric matrix. Considering $\boldsymbol{\mathcal{L}}(\tilde{\boldsymbol{L}}) = \boldsymbol{\mathcal{L}}(\boldsymbol{L}) + \boldsymbol{\mathcal{L}}(\boldsymbol{H})$, it is possible to obtain eigenvalues of $\boldsymbol{\mathcal{L}}(\tilde{\boldsymbol{L}})$ satisfying $\tilde{\lambda}_0 \geqslant 0$. $\boldsymbol{\mathcal{L}}(\tilde{\boldsymbol{L}})$ is a semipositive definite real symmetric matrix, whose Nm eigenvalues are $\lambda_1, \lambda_2, \cdots, \lambda_{Nm}$. Define $\boldsymbol{\xi} = (\xi_1, \xi_2, \cdots, \xi_{Nm}) \in \mathbf{R}^{Nm\times Nm}$ to be the orthogonal matrix of $\boldsymbol{\mathcal{L}}(\tilde{\boldsymbol{L}})$ and $\xi_1, \xi_2, \cdots, \xi_{Nm}$ to be the eigenvectors corresponding to the eigenvalues $\lambda_1, \lambda_2, \cdots, \lambda_{Nm}$, and obtain $\boldsymbol{\xi}^{\mathrm{T}}\boldsymbol{\xi} = \boldsymbol{\xi}\boldsymbol{\xi}^{\mathrm{T}} = \boldsymbol{I}_{Nm}$, where $\boldsymbol{I}_{Nm} \in \mathbf{R}^{Nm\times Nm}$ is the identity matrix. Then, it follows from real symmetric matrix properties that

$$\begin{aligned}&\frac{1}{2}(\boldsymbol{X}^1)^{\mathrm{T}}\boldsymbol{\mathcal{L}}(\tilde{\boldsymbol{L}})\boldsymbol{X}^1 = \frac{1}{2}(\boldsymbol{X}^1)^{\mathrm{T}}\boldsymbol{\xi}^{\mathrm{T}}\boldsymbol{\Lambda}\boldsymbol{\xi}\boldsymbol{X}^1 = \\ &\frac{1}{2}(\boldsymbol{X}^1)^{\mathrm{T}}\boldsymbol{\xi}^{\mathrm{T}}\boldsymbol{\Lambda}\boldsymbol{\xi}\boldsymbol{\xi}^{\mathrm{T}}\boldsymbol{\Lambda}^{-1}\boldsymbol{\xi}\boldsymbol{\xi}^{\mathrm{T}}\boldsymbol{\Lambda}\boldsymbol{\xi}\boldsymbol{X}^1 = \\ &\frac{1}{2}(\boldsymbol{X}^1)^{\mathrm{T}}\boldsymbol{\mathcal{L}}(\tilde{\boldsymbol{L}})\boldsymbol{\xi}^{\mathrm{T}}\boldsymbol{\Lambda}^{-1}\boldsymbol{\xi}\boldsymbol{\mathcal{L}}(\tilde{\boldsymbol{L}})\boldsymbol{X}^1 = \\ &\frac{1}{2}(\boldsymbol{Z}^1 + \boldsymbol{\varpi})^{\mathrm{T}}\boldsymbol{\Delta}(\boldsymbol{Z}^1 + \boldsymbol{\varpi}),\end{aligned} \tag{A8}$$

where $\boldsymbol{\Lambda} = \mathrm{diag}(\lambda_1, \lambda_2, \cdots, \lambda_{Nm})$ and $\boldsymbol{\Delta} = \boldsymbol{\xi}^{\mathrm{T}}\boldsymbol{\Lambda}^{-1}\boldsymbol{\xi}$.

Combining the Laplace matrix with the definition of the matrix $\boldsymbol{\mathcal{L}}(\tilde{\boldsymbol{L}})$ leads to

$$\frac{1}{2}(\boldsymbol{X}^1)^{\mathrm{T}}\boldsymbol{\mathcal{L}}(\tilde{\boldsymbol{L}})\boldsymbol{X}^1 = \frac{1}{2}(\boldsymbol{Z}^1 + \boldsymbol{\varpi})^{\mathrm{T}}\boldsymbol{X}^1. \tag{A9}$$

This concludes the proof.